phys. stat. sol. (b) **244**, No. 11, 3960–3963 (2007) / **DOI** 10.1002/pssb.200776148

Extreme thermal stability of carbon nanotubes

G. E. Begtrup[1,2], **K. G. Ray**[1,3], **B. M. Kessler**[1], **T. D. Yuzvinsky**[1,2,3], **H. Garcia**[1], and **A. Zettl**[*,1,2,3]

[1] Department of Physics, University of California at Berkeley, 94720 Berkeley, CA, USA
[2] Materials Sciences Division, Lawrence Berkeley National Laboratory, 94720 Berkeley, CA, USA
[3] Center of Integrated Nanomechanical Systems, 94720 Berkeley, CA, USA

Received 14 May 2007, revised 23 July 2007, accepted 21 September 2007
Published online 8 November 2007

PACS 65.80.+n, 81.07.De

The versatility of carbon–carbon bonding creates a wealth of extraordinary physical properties. Of the two common allotropes of carbon, diamond (sp-3 bonded) exhibits record thermal conductivity but is meta-stable and transits to graphite at elevated temperatures. Graphite (sp-2) is electrically conducting but sublimes at temperatures as low as 2400 K. Carbon nanotubes (also sp-2) capitalize on the extraordinary strength of the sp-2 hybridized carbon–carbon bond and exhibit high electrical and thermal conductivities as well as tremendous mechanical strength. Here we report a new technique to measure the thermal properties of nanosystems. We apply this technique to determine the ultimate high temperature breakdown of multiwalled carbon nanotubes.

1 Introduction

Although the electrical breakdown of carbon nanotubes in vacuum has been previously observed [1, 2], the temperature at which it occurs has not been directly measured, leaving the failure mechanism ambiguous. Theoretical studies predict extreme thermal stability of nanotubes up to 4000 K [3]. However, thermal measurements at these temperature extremes are very challenging, especially at the nanoscale. We apply a new technique to address these issues and to determine the ultimate failure temperature of electrically driven MWNTs in vacuum.

2 Thermal measurements of a MWNT

Figure 1a shows a conceptual drawing of the nanotube device. High quality arc discharge multiwalled carbon nanotubes (MWNTs) are ultrasonically dispersed in isopropanol and spin cast onto a suspended thin silicon nitride (Si_3N_4) membrane that is transparent to high energy electrons yet compatible with standard lithographic techniques [4]. This architecture allows real time high resolutions imaging of a device operating inside a transmission electron microscope (TEM). The MWNT is contacted using standard electron lithography followed by electron beam evaporation of 100 nm of palladium and liftoff in acetone. The nanotube devices typically exhibit low electrical resistance (~10 kΩ). Gold nanoparticles are then dispersed onto the device to act as single-shot thermometers as described below. These thermometers decorate the

[*] Corresponding author: e-mail: azettl@physics.berkeley.edu

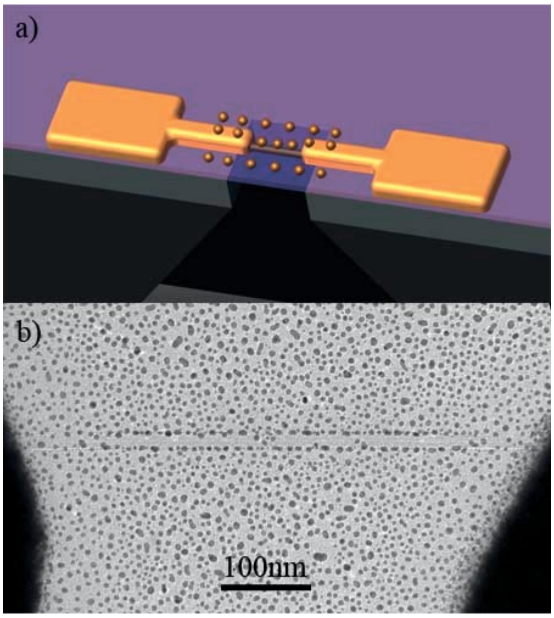

Fig. 1 (online colour at: www.pss-b.com) Nanotube thermal device. (a) Schematic of the device showing suspended Si_3N_4 membrane, nanotube, contacts, and nanoparticle thermometers. (b) Typical TEM image of a device prior to operation.

nanotube and the surrounding membrane. The discontinuous nanoparticle array is non-conductive and does not disrupt the transport properties of the nanotube. Figure 1b shows a corresponding TEM image of a typical device.

The thermal measurements are made by observing the melting and immediate evaporation of the gold nanoparticles decorating the system. We focus in particular on nanoparticles of diameter ~6 nm, which have a well-established melting temperature of 1275 K [5]. As the temperature of the sample rises, the nanoparticles evaporate, yielding the local temperature with nanoscale resolution.

Figure 2a shows the operation of a nanotube thermal device. The nanotube is electrically biased, causing Joule heating. The temperature of the center nanotube rises and heats the surrounding membrane.

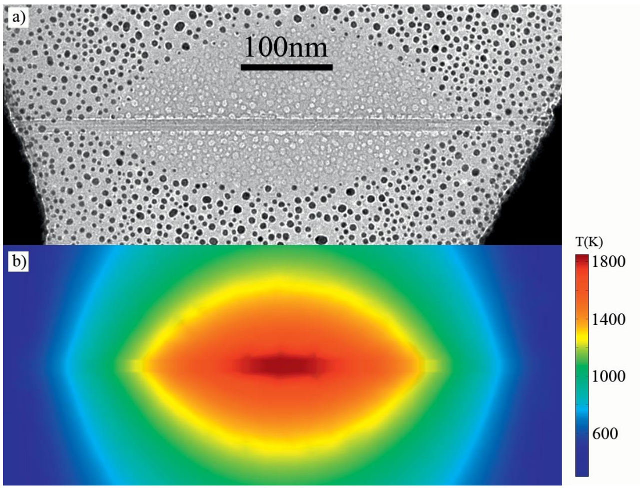

Fig. 2 (online colour at: www.pss-b.com) Operating the MWNT device. (a) TEM image of a MWNT device at high bias. The nanoparticles melt from the centre outward and create an isothermal line. (b) Model of the temperature distribution of the device in (a).

This process drives the melting and evaporation of the nanoparticle thermometers, which evaporate from the center of the device outward, indicating diffusive electrical conductivity of the nanotube. As the nanotube continues to heat, the thermometers melt further away from the center along the tube and on the membrane. This creates an isothermal line which fans out to steady states determined by the applied bias. The light coloured spots on the membrane are signatures of the evaporated thermometers, not holes in the membrane. The gold is completely removed.

3 Analysis

Figure 2b shows the modelled temperature profile of the device determined by finite element analysis. The steady state temperature profiles of the device are fit to the transport parameters, namely the applied bias and resistance. We solve the heat equation assuming diffusive conductivity in the nanotube (as demonstrated by the temperature of the device peaking in the centre). Treating the nanotube as a one-dimensional system with cross-section area A yields the heat equation:

$$A\,\nabla(\kappa\,\nabla T) + \frac{I \cdot V}{L} = 0\,, \tag{1}$$

where κ is the temperature dependent thermal conductivity, T the temperature, I the electrical bias current, V the voltage across the tube, and L the length of the tube. In the high temperature limit, nanotube thermal conductivity, incorporating both Umklapp and second-order 3-phonon processes [6], is described by:

$$\kappa(T) = \frac{1}{\alpha T + \beta T^2}\,, \tag{2}$$

with the linear term representing Umklapp (two-phonon) scattering and the quadratic term representing 3-phonon processes.

We self-consistently solve the system with appropriate boundary conditions and real materials parameters. The system is fit to two calibrations points, the melting of the gold nanoparticles thermometers at 1275 K at various steady states, and the eventual failure of the supporting Si_3N_4 membrane (described below) at 2173 K.

4 High temperature failure

Figure 3 shows the eventual failure of a MWNT device under extreme applied bias. Prior to failure, the supporting membrane fails at the centre of the device and slowly peels back with increasing bias. This provides an independent calibration temperature for the system, as Si_3N_4 dissociates at 2173 K. The sys-

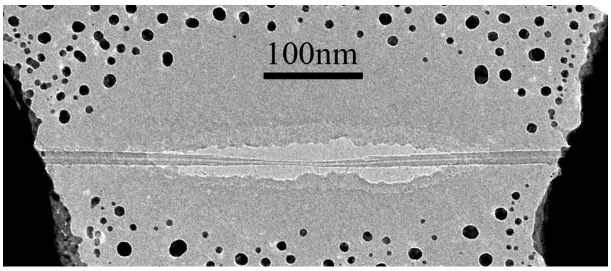

Fig. 3 High bias, high temperature failure of a MWNT. At significantly high bias, the supporting membrane dissociates and peels back. As the applied bias is further increased, the MWNT ultimately catastrophically fails wall by wall.

tem previously described is solved again with new appropriate boundary conditions (taking into consideration the deteriorated membrane) and new transport parameters immediately prior to failure. We determine the ultimate failure to be 3200 K, attributed to the onset of sublimation. This temperature approaches theoretical predictions [3] for nanotube stability and is 800 K higher than reported onset temperatures of sublimation of graphite [7, 8]. In addition, the electrical current density prior to failure for the MWNT of Fig. 2 (with inner diameter 4.8 nm and outer diameter 14.7 nm) is 1.7×10^8 A/cm^2. We thus find that nanotubes are the most robust form of carbon. This exceptional stability is attributed to the strength of the sp^2 bond and the relatively defect-free geometry of MWNTs.

Our thermal test platform as described could have many applications for exploring the thermal properties of novel nanomaterials and nanostructures. By applying the nanotube as a heater, non-conducting samples could similarly be studied. Furthermore, the extreme high temperature stability of carbon nanotubes presents exciting new applications.

Acknowledgements Financial support was provided by the U.S. National Science Foundation and the U.S. Department of Energy. Fellowship support was provided by the U.S. National Science Foundation for G.B. and by the U.S. Department of Defense for B.K. Funding for H.G. is provided by the University of California Chancellor's Fellowship.

References

[1] X. Cai, S. Akita, and Y. Nakayama, Thin Solid Films **464/465**, 364–367 (2004).
[2] J. Y. Huang, S. Chen, S. H. Jo et al., Phys. Rev. Lett. **94**, 236802 (2005).
[3] Y. Miyamoto, S. Berber, M. Yoon et al., Physica B **323**, 78–85 (2002).
[4] T. D. Yuzvinsky, W. Mickelson, S. Aloni et al., Appl. Phys. Lett. **87**, 083103 (2005).
[5] K. Koga, T. Ikeshoji, and K. I. Sugawara, Phys. Rev. Lett. **92**, 115507 (2004).
[6] N. Mingo and D. A. Broido, Nano Lett. **5**, 1221–1225 (2005).
[7] J. Haines and C. Tsai, Graphite Sublimation Tests for the Muon-Collider/Neutrino Factory Target Development Program, U.S. Department of Energy, Office of Science (2002).
[8] R. E. Honig, J. Chem. Phys. **22**, 126–131 (1954).

